Progress In Electromagnetics Research B, Vol. 22, 379–399, 2010

DESIGN OF A 60 GHz, 100 kW CW GYROTRON FOR PLASMA DIAGNOSTICS: GDS-V.01 SIMULATIONS

R. Jain and M. V. Kartikeyan

Department of Electronics and Computer Engineering
Indian Institute of Technology Roorkee
Roorkee 247 667, India

Abstract—In this work, the design studies of a 60 GHz, 100 kW CW gyrotron have been presented. Mode selection is carefully studied with the aim of minimizing mode competition and to yield a perfect solid beam output through an RF window with a suitable dimpled-wall quasi-optical launcher. Cavity design and interaction computations are then carried out. In addition, preliminary design of the magnetron injection gun, magnetic guidance system, launcher, and RF window are presented. Thus, we present a feasibility study, which indicates that the operation of such a gyrotron is possible and can give a power in excess of 100 kW at an efficiency $> 35\%$. As a part of this work, a complete Graphical User Interface package "GDS V.01" (Gyrotron Design Suit Ver.01) has been developed for the design and conceptualization of specific gyrotrons.

1. INTRODUCTION

Gyrotron oscillators (gyrotrons) are sources capable of delivering hundreds of kilowatts of power at microwave and millimeter wavelengths [1]. From their conception in the late fifties until their successful development for various applications, gyrotrons have come a long way technologically and made an irreversible impact on both users and developers. Gyrotron technology has significantly advanced during this time towards meeting the goals of providing a reliable and highly efficient source of high-power millimeter wave radiation.

Intense work on gyrotrons is being carried out for some important applications, first of all for heating of plasmas at nuclear fusion installations and high temperature processing of materials. These efforts have resulted in considerable progress from long pulses

Corresponding author: M. V. Kartikeyan (kartkfec@iitr.ernet.in).

Table 1. Design parameters and goals.

Frequency	60 GHz
Output power	$\approx$ 100 kW, CW
Diffraction Q (Q_D)	$\approx$ 1000
Beam current (I_b)	5–10 A
Accelerating voltage (U_b)	60–70 keV
Magnetic field (interaction)	$\approx$ 2.1–2.3 T
Velocity ratio (α)	$\approx$ 1.3
Total output efficiency	$\approx$ 35%
Estimated wall losses	$< 2.0\,\mathrm{kW/cm^2}$
Overall losses	$< 10\%$

to real CW regime at the highest output power as well as in considerable increase in efficiency of gyrotrons [2]. Plasma diagnostics in the millimeter/submillimeter wavelength range are valuable for the measurement of a wide range of plasma parameters including density, electron and ion temperatures, magnetic field direction, and non-thermal fluctuations [3]. Gyrotrons can make an important contribution to the advancement of these diagnostics. In this paper, the design studies of a 60 GHz, 100 kW, CW gyrotron for plasma diagnostics to be carried out in an experimental tokamak in India is presented. The design goals and specifications are summarized in Table 1.

During this course, the Graphical User Interface (GUI) package "GDS V.01" has been developed for the conceptual design of gyrotrons. The software incorporates the mode selection procedure, starting current calculations, gun synthesis and design of coils, resonator design and RF behavior computations, launcher design, non-linear taper design and finally the design RF-window. This package can be used to design a gyrotron with given specifications and goals.

2. GDS-V.01

"GDS V.01" (Gyrotron Design Suit Ver.01) has been developed for the feasibility and design of various modules/components of the gyrotron. It is a generalized design package which can be used to design a gyrotron with given specifications. This GUI has been developed in MATLAB R2006a. In this section the software has been explained and the design studies are discussed in the next sections along with the results.

The software starts with the mode selection procedure following [1]. Once the operating mode is selected the starting current calculations can be done to study mode competition. The starting current can be calculated in a linearized single-mode theory. This has been done in a number of ways by [1, 4–7], and will not be repeated here. The cold cavity computations are done following [1, 8–10]. Using these results self-consistent calculations can be carried out following [1, 10–12]. The theory and the equations describing gyrotron operation at arbitrary harmonics have been well known for a long time [1, 10–14]. Here, we use them in the form that was given in [1, 10], and do not repeat them. The results of the cavity design based on these single-mode self-consistent calculations [10, 12] are shown in Figs. 3–6. In addition, time-dependent self-consistent calculations [15] are also being added to this software, which is in progress at the time of preparation of this manuscript. The software also calculates the initial design values for MIG and magnetic guidance system following [1, 16, 17]. Optimized design of the MIG and magnetic guidance system can be carried out later using ESRAY [18]. Also, the initial design of non-linear taper can be carried out following [19, 20] and its final design optimization can be carried out later using a dedicated scattering matrix code [19, 21]. The initial design of quasi-optical launcher is calculated on the basis of [22–24] which can be later optimized using Launcher Optimization Tool [25]. Single disk and Double disk RF-windows can be designed following Nickel [1, 26]. Inclusion of the Brewster window design in the software is currently in progress.

Hence the software provides initial comprehensive data for the successful design of a gyrotron. These can be further optimized using the advanced codes available. In this manner all the procedures can be run and plots are also generated for the different profiles. The results in the subsequent sections have been calculated using the software GDS.

3. MODE SELECTION AND STARTING CURRENT CALCULATIONS

The given frequency corresponds to a free-space wavelength of 5 mm. As we very well know that in a gyrotron the electromagnetic radiation is produced in a TE mode near the cutoff frequency for that mode. For operation in the $\mathrm{TE_{m,p}}$ mode, the cavity radius is related to λ by $R_0 = \chi_{m,p}\lambda/(2\pi)$ where $\chi_{m,p}$ is the pth root of $J'_m(\chi) = 0$. For operation at the first harmonic ($s = 1$) the optimum electron beam radius is given by $R_b = \chi_{m\pm1,i}R_0/\chi_{m,p} = \chi_{m\pm1,i}\lambda/(2\pi)$, ($i = 1$ or 2). In general, the corotating mode (with the lower sign) is chosen, since this provides better coupling of the electron beam to the RF-field.

In the mode selection procedure, all the modes with eigenvalues ranging from 8 to 18 were inspected (as matter of experience). In addition to the satisfactory evaluation of the modes that are meeting the general design considerations (such as peak wall loading, voltage depression, limiting current, etc.), the candidate modes should also support an advanced dimpled wall launcher of the quasi-optical output coupler. Only well qualified modes are selected for this feasibility study. The values of the design constraints of each of these modes are calculated as shown in Table 2. Three modes, namely $TE_{5,2}$, $TE_{6,2}$ and $TE_{7,2}$, were found to be within the design constraints. But to fulfill the requirements of the advanced dimpled-wall quasi-optical launcher, $TE_{6,2}$ mode was found to be the best candidate.

As a next step, the starting currents have been computed for this candidate mode and possible competing modes that might prevent operation in the desired mode. The starting currents for a $TE_{6,2}$ mode gyrotron operating at 60 GHz along with its competing modes are shown in Fig. 1. A Gaussian field profile was employed for these calculations, which is a common practice to initially compute the starting currents of main mode and its competitors to have a preliminary assessment. By inspection of the starting current curves that were computed for the candidate mode and possible competing modes, as shown in Fig. 1, it became clear that the $TE_{6,2}$ mode was best separated from possible competing modes. Also during the mode selection process we have seen that this mode satisfies all technical design constraints within the limits. Hence this mode has been considered as operating mode for further studies.

Table 2. Azimuthal index, radial index, mode eigenvalue, cavity radius, beam radius, voltage depression, limiting current, peak-wall loading, and $m_2/2(= 360/\phi)$ for probable candidate modes for a 60 GHz gyrotron.

m	p	$\chi_{m,p}$	R_0 mm	R_b mm	V_d kV	I_L A	dP/dA kW/cm^2	$m_2/2$
0	3	10.173469	8.10	1.47	1.88	23.7	.060	2.00
3	2	8.015237	6.38	2.43	1.06	42.0	.113	2.65
3	3	11.345925	9.03	2.43	1.45	30.9	.052	2.41
4	2	9.282396	7.39	3.34	.87	51.1	.089	2.79
4	3	12.681909	10.09	3.34	1.22	36.7	.043	2.51
5	2	10.519861	8.37	4.23	.75	59.4	.073	2.92
6	2	11.734936	9.34	5.11	.67	67.1	.061	3.04
7	2	12.932386	10.29	5.97	.60	74.4	.053	3.15

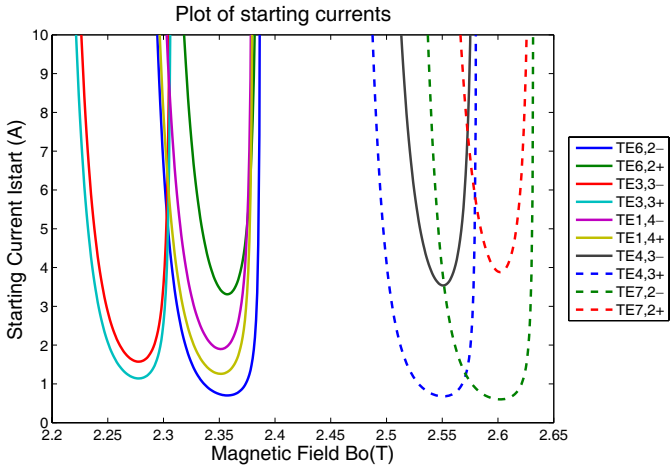

Figure 1. Starting current I_{start} as a function of magnetic field B_0 for various modes with beam radius (R_b) optimized for the $TE_{6,2}$ mode at 60 GHz, with accelerating voltage $U_0 = 65\,\text{kV}$, $\alpha = 1.3$, $R_0 = 9.34\,\text{mm}$, $R_b = 5.11\,\text{mm}$, and $Q_D = 954$.

4. RF BEHAVIOR

The optimum cavity design is carried out by computing the power and interaction efficiencies in cold cavity and self-consistent approximations for various parameters until a satisfactory cavity design compatible with the design goals such as efficiency, wall losses, output power etc. is obtained.

4.1. Cold-cavity Design Calculations

The cavity is a standard three section structure with an input taper and a uniform mid-section followed by an output upward taper. The beam-wave interaction takes place in the uniform mid-section where the RF-field reaches peak values. The external magnetic field starts to decrease in the up-taper region which results in residual interaction that sometimes causes a loss of efficiency. Therefore the output taper has not been included as a part of resonator geometry.

For the $TE_{6,2}$ mode at 60 GHz, the cavity radius is 9.34 mm and beam radius is 5.11 mm. For cavities with moderate quality factors, the length parameter of the Gaussian field profile L is generally taken between $7\lambda \leq L \leq 8\lambda$, where λ is the free space wavelength. As the wavelength is 5 mm, it gives a diffractive quality factor $Q_D \approx 900$. We

Table 3. Interaction cavity data.

L_2 (mm)	f (GHz)	Q_D
34	60.0290	825
35	60.024	888
36	60.019	954
37	60.015	1023
38	60.011	1095

Table 4. Final design of the cold-cavity.

R_1	8.03 mm
R_2	9.34 mm
R_3	11.436 mm
L_1	30 mm
L_2	36 mm
L_3	40 mm
θ_1	2.5°
θ_2	0°
θ_3	3.0°
D_1	10 mm
D_2	10 mm
Q_{Diff}	954

have varied the cavity mid-section length over the range and obtained the data as shown in Table 3. After a careful study of the various sets of results obtained keeping in mind the goals defined, a cavity midsection length of 36 mm was selected as it gives a $Q_D = 954$. The wall losses become too high for greater quality factors. The final cavity data has been depicted in Table 4. Fig. 2 shows the cold-cavity field profile, as well as the cavity geometry for $L_2 = 36$ mm.

The output of these cold cavity calculations is further used in self-consistent computations to evaluate power and efficiencies.

4.2. Self-consistent Calculations

Self-consistent calculations [1, 10] for power and efficiency are carried out for a range of external parameters, namely: beam energy,

beam velocity ratio α, beam current and applied magnetic field. Computations are carried out for three cavity mid-section lengths $L_2 = 34.0/36.0/38.0\,\text{mm}$ that give values of $Q_D = 825/954/1095$ respectively.

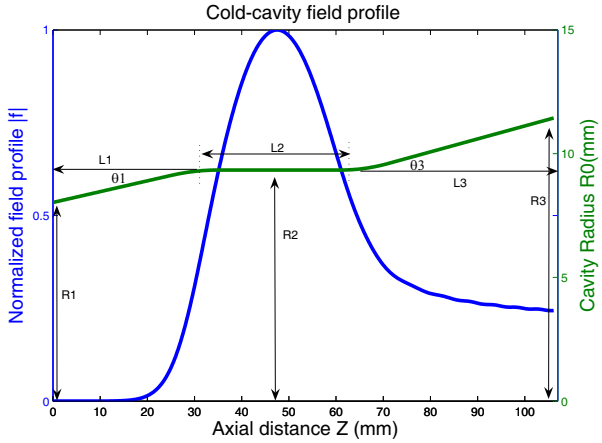

Figure 2. Final cold-cavity field profile.

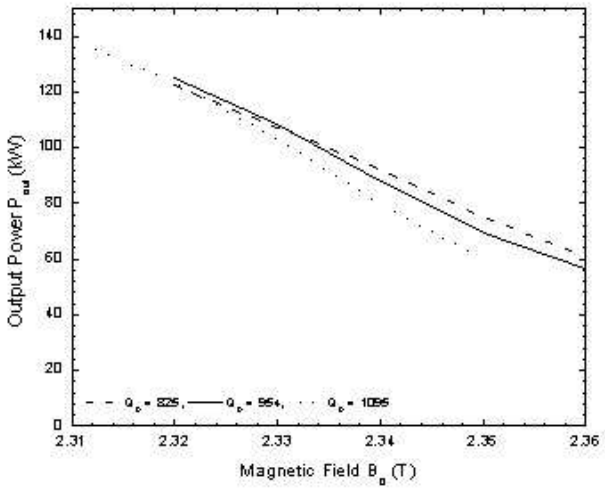

Figure 3. Output power as a function of cavity magnetic field (B_0) with: $U_B = 65\,\text{kV}$, $I_B = 5\,\text{A}$, and $\alpha = 1.3$.

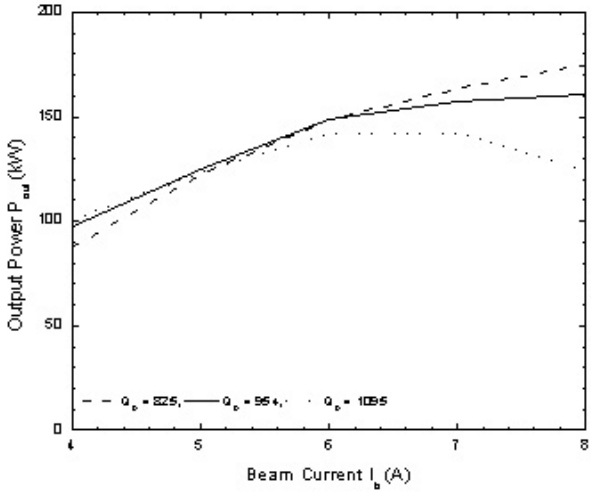

Figure 4. Output power as a function of beam current (I_B) with: $U_B = 65\,\text{kV}$, $B_0 = 2.32\,\text{T}$, and $\alpha = 1.3$.

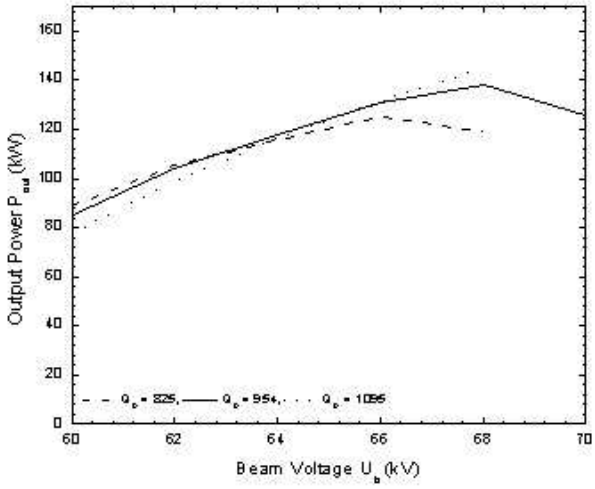

Figure 5. Output power as a function of beam voltage (U_B) with: $I_B = 5\,\text{A}$, $B_0 = 2.32\,\text{T}$, and $\alpha = 1.3$.

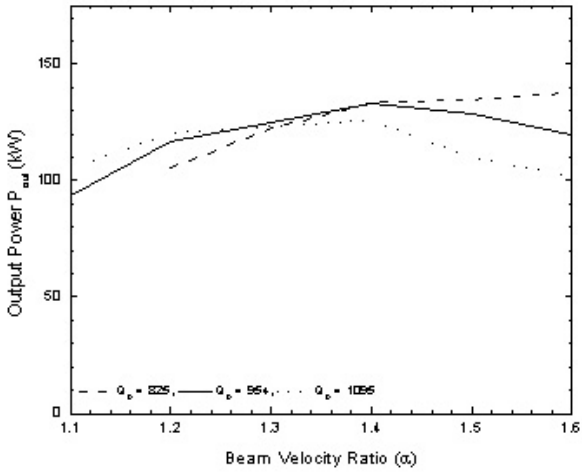

Figure 6. Output power as a function of beam velocity ratio (α) with: $U_B = 65\,\text{kV}$, $I_B = 5\,\text{A}$, and $B_0 = 2.32\,\text{T}$.

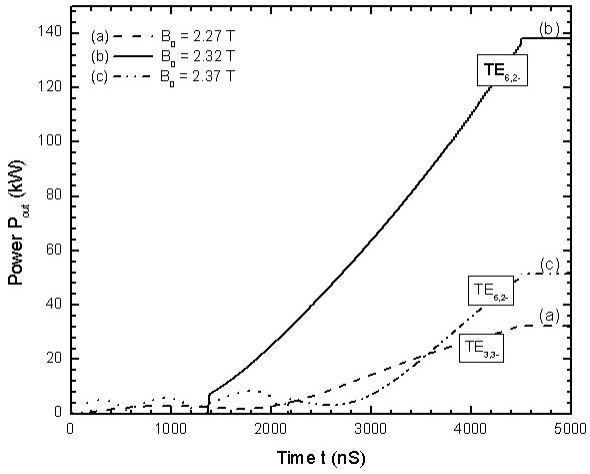

Figure 7. SELFT simulation results for a $TE_{6,2}$ gyrotron considering the probable competing modes. (a) $B_0 = 2.27\,\text{T}$, (b) $B_0 = 2.32\,\text{T}$ and (c) $B_0 = 2.37\,\text{T}$.

However, from the design goals and the computations done, it is obvious that one can conveniently consider the cavity geometry corresponding to $Q_D = 954$ as the best choice to carry out the interaction computation. The results of the cavity design based on self-consistent computations are shown in Figs. 3–6. From these figures, it is evident that operation at the fundamental ($s = 1$) at 60 GHz with the $TE_{6,2}$ mode as the operating mode gives well above 100 kW of cavity output power with around 38% efficiency. Calculated maximum wall losses are 0.5 kW/cm^2 at 100 kW.

In addition, time-dependent self-consistent (SELFT) calculations [15] are carried out for the cavity geometry with $Q_D = 954$ considering all the probable competing modes. Fig. 7 shows the results of a simulation with SELFT for the $TE_{6,2}$ mode along with probable competing modes. In these calculations, the beam energy is increased from 40 keV to 65 keV over a fictitious startup time of 5000 ns, and the velocity ratio varies accordingly. The beam current and magnetic field are held constant. The computations are carried out for three different magnetic fields (B_0(T) = 2.27, 2.32, 2.37). If the magnetic field remains constant at 2.32 T, then the $TE_{6,2}$ mode oscillates well. These results indicate that stable operation of a gyrotron in the $TE_{6,2}$ mode at 60 GHz at power levels in excess of 100 kW should be possible.

5. MIG AND GUIDANCE SYSTEM

The magnetic guidance system is a very important step in the design of gyrotrons. A rough estimation of the device length can be made by looking at the magnetic field profile. Magnetic field profile data are needed to perform precise simulation studies on magnetron injection gun and RF-behavioral aspects. In addition, it is required for collector design. Most gyrotrons employ solenoids (either superconducting or normal conducting coils) to provide necessary magnetic field for beam guidance from the cathode through interaction region up to the collector. In this section, the design of a magnetic guidance system required for a 60 GHz, 100 kW, CW gyrotron is presented.

A simple and cost effective magnet design can be achieved using a single coil which gives the maximum required field at the center of the cavity and uses the stray field in the gun and collector region. However, in a more effective design of the magnetic guidance system employed here, we have used a radially tapered main coil (modeled by a single main coil and two auxiliary coils) and one gun coil. The coil data has been calculated using [17] and shown in Table 5. This initial data obtained from GDS is then optimized using [18]. The axial magnetic field with the proposed coil arrangement with gun geometry is shown

Table 5. Coil data.

Coil	ΔZ (mm)	ΔR (mm)	N_C	I_C (Amp)
Main Coil-1	360.00	15.00	9920	72
Main Coil-2	90.00	7.50	630	72
Main Coil-3	90.00	7.50	630	72
Gun Coil	20.00	15.00	610	−49.5

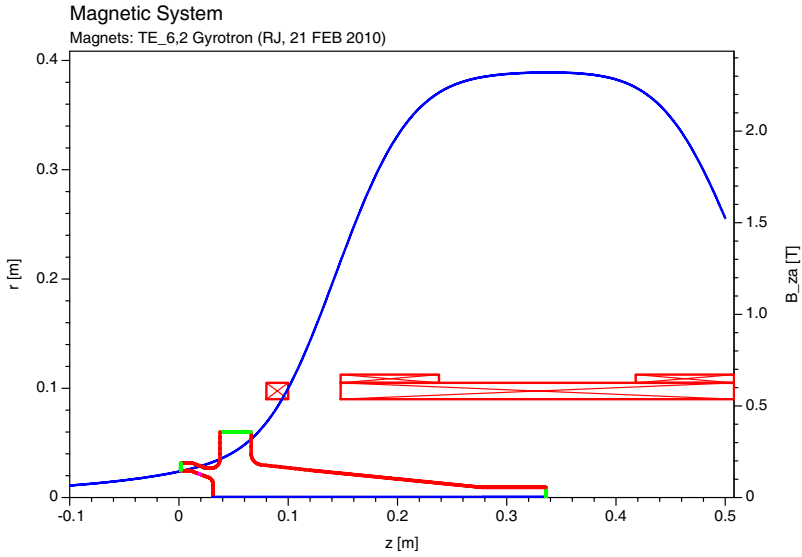

Figure 8. Axial magnetic field profile of the coils.

in Fig. 8. It is also possible to use a normal (not superconducting) electromagnet. Alternatively, a Helmholtz coil arrangement could be used.

For the $TE_{6,2}$ mode operating at the first harmonic, the beam radius is 5.11 mm. Assuming a compression ratio of approximately 18, gives a cathode radius of approximately 21.5 mm. The accelerating voltage should be in the range 65–70 kV, and the velocity ratio approximately 1.2–1.4. Simple adiabatic theory, leading to the Baird-Lawson equations [16] indicates that, for a triode-type gun, and parameters as given above, the anode-cathode spacing would be rather large. Under adiabatic approximation, the electron motion in crossed electric and magnetic fields can be separated into a gyration motion

of the electrons and a drift of their guiding centers [1]. This adiabatic approximation is valid if the electric and magnetic fields are rather small at dimensions characteristic for the electron trajectories.

More recently, the use of cusp or pierce gun along with a kicker to obtain transverse velocity for gyrotrons/gyro-devices has been proposed in [27–29]. However, we have used a Magnetron Injection Gun (MIG). As a matter of convenience and flexibility, a triode version of the MIG has been proposed. In addition, it provides more possibilities to control beam parameters. However, a diode type MIG is simpler to realize. Assuming a compression ratio of about 18, the design data have been prepared and are shown in Table 6. The initial design was obtained following a simple adiabatic theory, leading to the Baird-Lawson equations [16]. The design is then refined using the ESRAY code [18].

Figure 9 shows the geometry of the gun and the particle trajectories for one of the optimized runs of ESRAY. Typical beam properties obtained for a compression of $b = 18$ are fairly good and are $U_b = 66.06\,\text{kV}$, $\alpha = 1.2925$, $\beta_\perp = 0.367$, $\Delta\alpha/\alpha = 5.788\%$, with $U_{mod} = 34.0\,\text{kV}$ and $I_b = 10\,\text{A}$. It is noted that the velocity spread increases significantly for higher values of U_{mod}, mainly due to the larger values of $\beta_\perp$ for electrons emitted from the outside edges of the emitter.

Table 6. Preliminary design data of triode type MIG.

Beam current	5–10 A
Accelerating voltage	$\approx 67\,\text{kV}$
Compression ratio	18
Beam radius (interaction)	5.11 mm
Larmor radius (interaction)	0.308 mm
Cathode radius	21.02 mm
Cathode angle	20.8°
Anode angle	20.8°
Cathode slant length	3.52 mm
Emitter current density	$2.1\,\text{A/cm}^2$
Cathode-anode clearance	9.77 mm
Velocity ratio α	1.2–1.4
Electric field at cathode	4.2 kV/mm

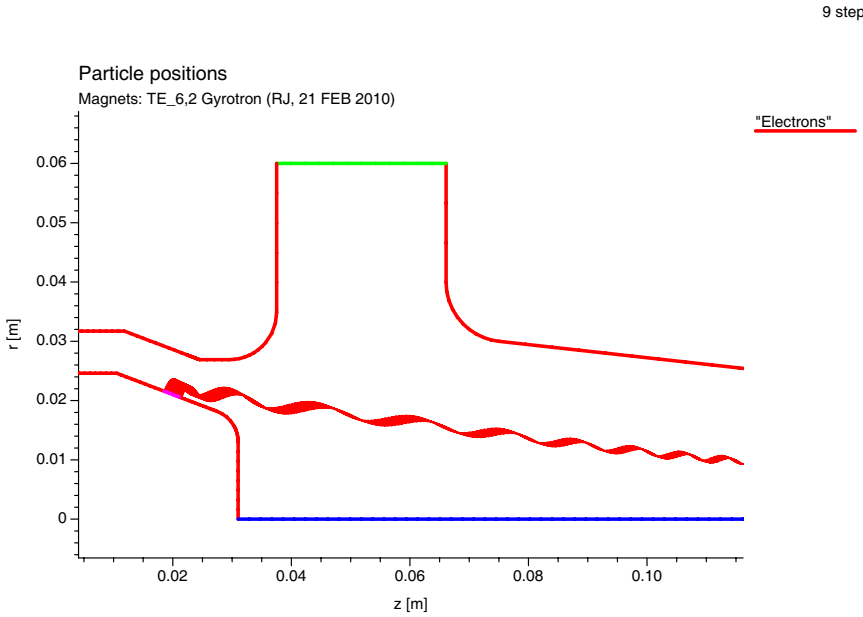

Figure 9. Triode type MIG with particle trajectories.

6. OUTPUT SYSTEM

Gyrotron output systems consist of an output diameter taper which connects the interaction region with the main waveguide system, a quasi-optical mode converter, and the RF window [1].

6.1. Non-linear Taper

The requirement of a diameter taper in gyrotrons is to provide a good match between input and output sections of the taper with very low spurious mode content. In gyrotrons, cross-section taper, in general of cylindrical type, are employed between the output section of the cavity to the main waveguide section. Cross-section tapers should not generate spurious modes above a certain acceptable level.

In this work, a raised cosine taper profile has been used as it yields very low mode conversion. The analysis of the taper was carried out using a dedicated scattering matrix code as it is very fast and accurate for taper analysis [19]. The parameters of the non-linear taper are — the length of the taper (L), the radius of the taper at input end (r_1), the radius of the taper at the output end (r_2), the number of sections to be discredited (N), and a geometrical parameter gamma (γ). L, N

Table 7. Final design of nonlinear taper.

r_1	11.436 mm
r_2	13.100 mm
L	100.00 mm
γ	0.67
N	350
S_{21}	99.6087%

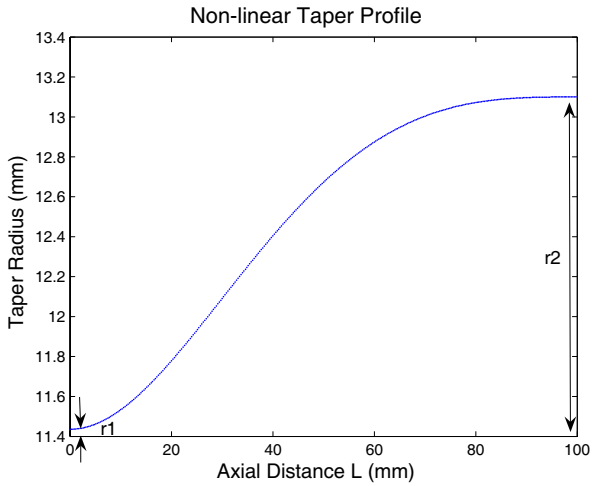

Figure 10. Final profile of the designed nonlinear taper. The design values are given in Table 7.

and γ are varied while keeping r_1 and r_2 constant to achieve maximum transmission. The values of the design parameters considered for the design are summarized in Table 7. The objective of the design was to obtain a maximum transmission coefficient (i.e., S_{21}-parameter), operating with $TE_{6,2}$ mode with minimized spurious mode content. Finally, taper contour profile along its length is appreciated graphically in Fig. 10. This non-linear taper can further be optimized as in [20] if required.

6.2. Quasi-optical Launcher

The advanced mode converter employs a dimpled-wall waveguide section and a helical-cut launching aperture as an antenna, one quasi-

elliptical mirror and two toroidal mirrors as beam-forming mirror system. The role of the dimpled-wall waveguide antenna is to transform the gyrotron cavity mode into a bundle of modes that form a Gaussian intensity profile at the aperture, prior to the reflectors. These wall distortions (scattering surface) can transform the input eigenwave to an eigenwave of the weakly perturbed transmission line. That beam is appropriate to be used directly as a free space TEM_{00} mode, or to be transmitted as a low-loss hybrid HE_{11} mode in highly over-moded corrugated waveguides [22–24, 30, 31]. The surface deformation points on type-2 surface are calculated on the basis of the studies given by Hirata [30]. The deformation points are optimized to maximize the Gaussian content in the beam at the helical cut.

For the current gyrotron operating at the $TE_{6,2}$ cavity mode the design achieved 99.60% conversion efficiency from high order waveguide modes to Gaussian-like beams in free space, allowing them to be used in high power gyrotrons. QO launcher radiation pattern is simulated and optimized using Launcher Optimization Tool (LOT). The launcher parameters are given in Table 8. These parameters are optimized using LOT.

The first step is to take only 2 sets of perturbations on type-2 surface and optimize to get the maximum Gaussian fit. Then one more set of perturbation is included in the optimized file and again maximum Gaussian fit needs to be achieved. Same process is followed one more time to have four sets of perturbations in the same surface file on type-2 surface. Finally the surface is converted to type-3 surface using the surface converter and then optimized. The final Gaussian fit obtained using this design is 99.60% for the $TE_{6,2}$ mode. The wall field intensity and aperture field intensity obtained on type-3 surface after optimization using the Launcher Optimization Tool with four deformations are shown in Fig. 11 and Fig. 12 respectively.

6.3. RF Window

The RF window is a critical component that transmits the output power to the external system. It must withstand high power,

Table 8. Launcher parameters.

Launcher Length	215 mm
Helical Cut Length	60 mm
Waveguide Radius	13.10 mm
Taper Angle	0.004°

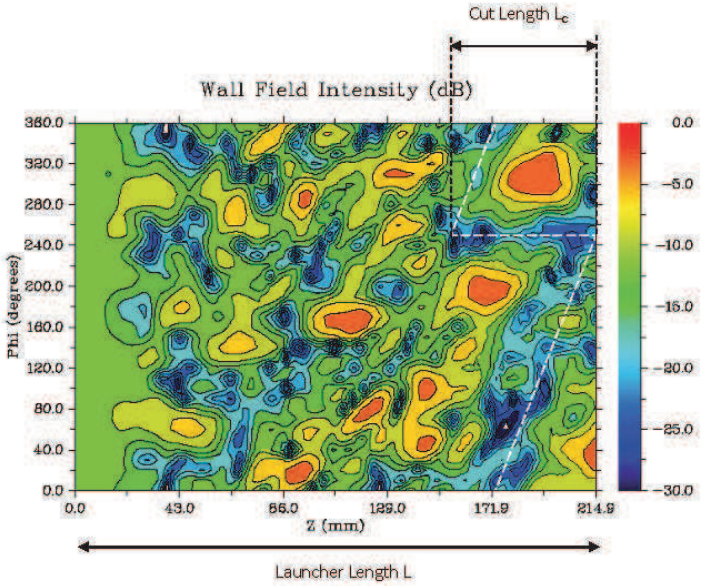

Figure 11. Wall field intensity of launcher.

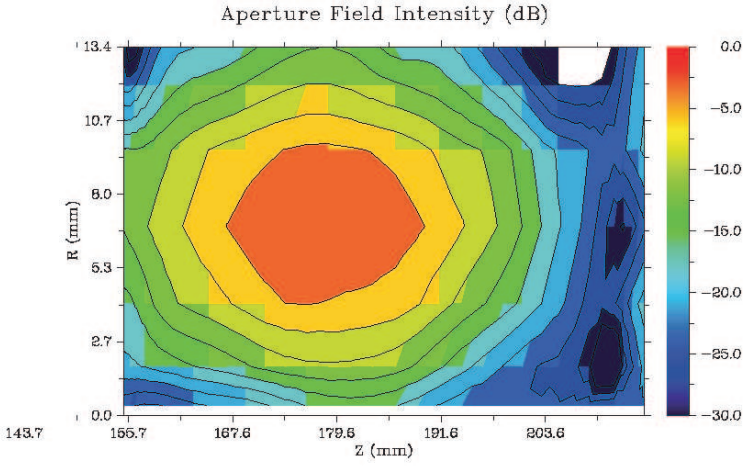

Figure 12. Aperture field intensity of launcher.

mechanical stresses, and pressure gradients. Therefore, care must be taken in selecting the proper window material with low-loss tangent, high thermal conductivity, and mechanical strength since the window must withstand large thermal and mechanical stresses. Ideally, it should also offer easy metallization/ brazing and make a strong vacuum-tight seal with metals.

The state-of-the-art of window materials for high-power gyrotrons is described in [2, 32]. For high-power CW gyrotrons at millimetric wavelengths, advanced materials such as sapphire, CVD diamond, Au-doped silicon, etc., have to be used. For the current conceptual design, a double disk window has been designed with sapphire as the window material. The window design is carried out for a Gaussian beam with radial output coupling with an estimated window aperture radius of 50 mm (approximately 1.67 times the Gaussian beam radius). The dimensions of both the disks are kept same. The design values are

Table 9. Design values for double disk window.

Window aperture radius	50 mm
Disk thickness (D_1 and D_2)	2.447 mm
Disk Permittivity	9.41
Loss Tangent of disk	5.56×10^{-5}
Coolant Permittivity	1.8
Loss Tangent of coolant	26×10^{-4}

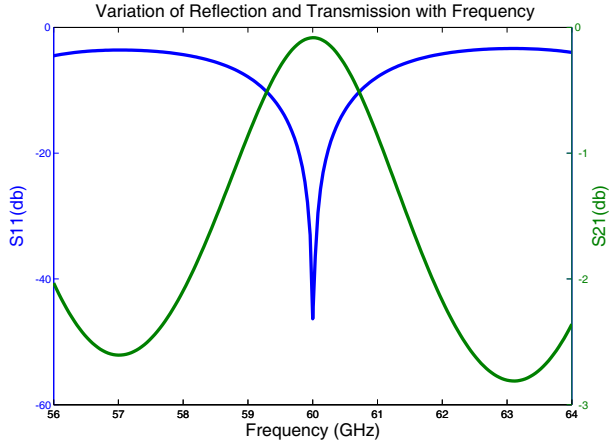

Figure 13. Transmission and reflection characteristics of the window.

given in Table 9. The variation of the reflection and transmission with frequency for this design are as shown in Fig. 13. A transmission of 98.127% has been achieved for the design values in Table 9.

7. CONCLUSIONS AND OUTLOOK

This work presents a design of a 60 GHz, 100 kW conventional cavity gyrotron operating in the $TE_{6,2}$ mode. The feasibility of such a gyrotron with an output power in excess of 100 kW at nearly 38% efficiency has been confirmed theoretically. The main application of this specific gyrotron is for plasma diagnostics in India. Gyrotron design software GDS V.01 has been developed.

Version 02 of the software is on its way which includes the time-dependent self consistent calculations [15] and space charge effects [33]. It will also include the option of designing a Brewster window. This software will prove very helpful in calculating the initial comprehensive data for the design of specific gyrotrons.

ACKNOWLEDGMENT

The authors sincerely thank Prof. Dr. Manfred Thumm (Director, IHM, Karlsruhe Institute of Technology, Karlsruhe, Germany) for his valuable suggestions, cooperation and critical reading of the manuscript. The authors wish to thank Prof. E. Borie, Dr. Stefan Illy, Dr. Stefan Kern, and Dr. D. Wagner for their help and cooperation.

REFERENCES

1. Kartikeyan, M. V., E. Borie, and M. Thumm, *Gyrotrons — High Power Microwave and Millimeter Wave Technology*, Springer-Verlag, Berlin-Heidelberg, Germany, 2004.
2. Thumm, M., *State-of-the-art of High Power Gyro-devices and Free Electron Masers Update 2008*, Scientific Report FZKA 7467, Forschungszentrum Karlsruhe, Germany, Apr. 2009.
3. Woskoboinikow, P., "Development of gyrotrons for plasma diagnostics," *Review of Scientific Instruments*, Mar. 1986.
4. Petelin, M. I., "Self-excitation of oscillations in a gyrotron," *Inst. Appl. Phys.*, in Gyrotrons: Collected Papers, USSR Academy of Sciences, Gorki, Russia, 1981.
5. Kreischer, K. E. and R. J. Temkin, "Linear theory of an electron cyclotron maser operating at the fundamental," *Int. J. Infrared Millim. Waves*, Vol. 1, No. 2, 195–223, Jun. 1980.

6. Nusinovich, G. S., "Linear theory of a gyrotron with weakly tapered external magnetic field," *Int. J. Electron.*, Vol. 64, No. 1, 127–136, Jan. 1988.
7. Borie, E. and B. Jdicke, "Comments on the linear theory of the gyrotron," *IEEE Trans. Plasma Sci.*, Vol. 16, No. 2, 116–121, Aug. 1988.
8. Fliflet, A. W. and M. E. Read, "Use of weakly irregular waveguide theory to calculate eigenfrequencies, Q-values and RF field functions for gyrotron oscillators," *Int. J. Electronics*, Vol. 51, 475–484, 1981.
9. Borie, E. and O. Dumbrajs, "Calculation of eigenmodes of tapered gyrotron resonators," *Int. J. Electronics*, Vol. 60, 143–154, 1986.
10. Borie, E., *Gyrotron Oscillators: Their Principles and Practice*, edited by C. J. Edgcombe, Ch. 3, Taylor & Francis, London, 1993.
11. Fliflet, A. W., M. E. Read, K. R. Chu, and R. Seeley, "A self-consistent field theory for gyrotron oscillators: Application to a low Q gyromonotron," *Int. J. Electronics*, Vol. 53, 505–521, 1982.
12. Borie, E., B. Jodicke, and O. Dumbrajs, "Self consistent code for a 150 GHz gyrotron," *Int. J. Electronics*, Vol. 7, 1863–1879, 1986.
13. Bratman, V. L., M. A. Moiseev, M. I. Petelin, and R. E. Erm, "Theory of gyrotrons with a non-fixed structure of the high-frequency field," *Radiophys. Quantum Electron.*, Vol. 16, No. 4, 474–480, Apr. 1973.
14. Bratman, V. L., M. A. Moiseev, and M. I. Petelin, "Theory of gyrotrons with low-Q electromagnetic systems," *Inst. Appl. Phys.*, in Gyrotrons: Collected Papers, USSR Academy of Sciences, Gorki, Russia, 1981.
15. Kern, S., "Numerische Simulation der Gyrotron-Wechselwirkung in koaxialen Resonatoren," Scientific Rep. FZKA 5837, Forschungszentrum Karlsruhe, Nov. 1996.
16. Baird, J. M. and W. Lawson, "Magnetron injection gun (MIG) design for gyrotron applications," *Int. J. Electronics*, Vol. 61, 969–984, 1986.
17. Vaughan, J. R. M., "Representation of axisymmetric magnetic fields in computer programs," *IEEE Transactions on Electron. Devices*, Vol. 19, 144, 1972.
18. Illy, S., "ESRAY — A computer code for the analysis of axisymmetric electron guns," *Private Communication*, 2002.

19. Wagner, D., M. Thumm, G. Gantenbein, W. Kasperek, and T. Idehara, "Analysis of a complete gyrotrons oscillator using the scattering matrix description," *Int. J. Infrared Millimeter Waves*, Vol. 19, No. 2, 185–194, 1998.
20. Chauhan, N., A. Mittal, D. Wagner, M. V. Kartikeyan, and M. Thumm, "Design and optimization of nonlinear tapers using particle swarm optimization," *Int. J. Infrared* & Millimeter Waves, Vol. 29, No. 8, 792–798, Aug. 2008.
21. Cascade scattering matrix Code, v 3.0, Calabazas Creek Research Inc., 2000.
22. Thumm, M., "Modes and mode conversion in microwave devices," *Generation and Application of High Power Microwaves*, R. A. Cairns and A. D. R. Phelps (eds.), IOP, Bristol, U.K., 121–171, 1997.
23. Jin, J., "Quasi-optical mode converter for a coaxial cavity gyrotron," Wissenschaftliche Berichte, FZKA 7264, Karlsruhe, Mar. 2007.
24. Jin, J., B. Piosczyk, M. Thumm, T. Rzesnicki, and S. Zhang, "Quasi-optical mode converter/mirror system for a high power coaxial-cavity gyrotron," *IEEE Transactions on Plasma Science*, Vol. 34, No. 4, 1508–1515, Aug. 2006.
25. Launcher Optimization Tool, User Manual, Version 1.21, Calabazas Creek Research, Inc., 2006.
26. Nickel, H.-U., "Aspects of high frequency technology for the development of low-reflection output windows for high power millimeter-wave gyrotrons," Sci. Rep. FZKA 5513, Forschungszentrum Karlsruhe, Karlsruhe, Germany, 1995.
27. He, W., C. G. Whyte, E. G. Rafferty, A. W. Cross, A. D. R. Phelps, K. Ronald, A. R. Young, C. W. Robertson, D. C. Speirs, and David Rowlands, "Axis-encircling electron beam generation using a smooth magnetic cusp for gyrodevices," *Appl. Phys. Lett.*, Vol. 93, 121501, 2008.
28. Donaldson, C. R., W. He, A. W. Cross, F. Li, A. D. R. Phelps, L. Zhang, K. Ronald, C. W. Robertson, C. G. Whyte, and A. R. Young, "A cusp electron gun for millimeter wave gyrodevices," *Appl. Phys. Lett.*, Vol. 96, 141501, 2010.
29. Cooke, S. J., A. W. Cross, W. He, and A. D. R. Phelps, "Experimental operation of a cyclotron autoresonance maser oscillator at the second harmonic," *Phys. Rev. Lett.*, Vol. 77, 4836–4839, 1996.
30. Hirata, Y., Y. Mitsunaka, K. Hayashi, Y. Itoh, K. Sakamoto,

and T. Imai, "The design of a tapered dimple-type mode converter/launcher for high-power gyrotrons," *IEEE Transactions on Plasma Science*, Vol. 31, No. 1, 142–145, Feb. 2003.

31. Neilson, J. M., "Optimal synthesis of quasi-optical launchers for high-power gyrotrons," *IEEE Transactions on Plasma Science*, Vol. 34, No. 3, 635–641, Jun. 2006.
32. Thumm, M., "Development of output windows for high power long pulse gyrotrons and EC wave applications," *Int. J. Infrared Millim. Waves*, Vol. 19, 3–14, 1998.
33. Borie, E. and S. Kern, "On the effect of RF-space charge on the beam-field interaction in gyrotrons," *J. Infrared Milli. Terahz Waves*, Vol. 30, 915–923, 2009.